Thermal Axions: Production Mechanisms and Cosmological Signals

Francesco D'Eramo[1,2]

[1]*Dipartimento di Fisica e Astronomia, Università degli Studi di Padova, Via Marzolo 8, 35131 Padova, Italy*
[2]*Istituto Nazionale di Fisica Nucleare (INFN), Sezione di Padova, Via Marzolo 8, 35131 Padova, Italy*

Abstract

Scattering and decay processes of thermal bath particles in the early universe can dump relativistic axions in the primordial plasma. If produced with a significant abundance, their presence can leave observable signatures in cosmological observables probing both the early and the late universe. We focus on the QCD axion and present recent and significant improvements for the calculation of the axion production rate across the different energy scales during the expansion of the universe. We apply these rates to predict the abundance of produced axions and to derive the latest cosmological bounds on the axion mass and couplings.

Keywords: axions, early universe, dark radiation
DOI: 10.31526/LHEP.2023.353

1. INTRODUCTION

The Peccei-Quinn (PQ) mechanism [1, 2] is an elegant solution to the experimentally observed invariance of strong interactions when we flip the arrow of time. For each microscopic realization, the framework features a global symmetry $U(1)_{\rm PQ}$ that must satisfy two key requirements: spontaneously broken, and anomalous under the color gauge group of the standard model. The scale of spontaneous PQ breaking is bound to be much higher than the energies experimentally accessible, and the only low-energy residual is a pseudo-Nambu-Goldstone boson (PNGB) known as the QCD axion [3, 4]. The color anomaly imposes a coupling of the axion field a to gluons via the dimension 5 operator:

$$\mathcal{L}_{\rm PQ} \supset \frac{\alpha_s}{8\pi}\frac{a}{f_a}G^A_{\mu\nu}\widetilde{G}^{A\mu\nu}. \tag{1}$$

This operator defines the axion decay constant f_a. We have above the QCD fine structure constant $\alpha_s = g_s^2/(4\pi)$, the gluon field strength tensor $G^a_{\mu\nu}$, and its dual $\widetilde{G}^{a\mu\nu}$. Interactions with other standard model fields are model dependent, and given its PNGB nature, all axion couplings are suppressed by the scale f_a. Broadly speaking, there are two classes of axion couplings to visible matter:

$$\mathcal{L}_{\rm axion-int} \supset \frac{1}{f_a}\left[ac_X\frac{\alpha_X}{8\pi}X^{a\mu\nu}\widetilde{X}^a_{\mu\nu} + \partial_\mu a c_\psi \overline{\psi}\gamma^\mu\psi\right]. \tag{2}$$

The first class contains couplings to standard model gauge bosons ($X = \{G, W, B\}$), and we set $c_G = 1$ consistently with equation (1). The standard model fermions appearing in the second class have defined electroweak quantum numbers ($\psi = \{Q_L, u_R, d_R, L_L, e_R\}$), and their interactions preserve the shift symmetry $a \to a + \text{const}$. QCD non-perturbative effects generate a potential once strong interactions confine, and this leads to an axion mass [5]:

$$m_a \simeq 5.7\,\mu\text{eV}\left(\frac{10^{12}\,\text{GeV}}{f_a}\right). \tag{3}$$

Famously, the QCD axion is a viable dark matter candidate [6, 7, 8] as reviewed in Section 2. We focus on thermal axions in Section 3, and we give updated predictions for the KSVZ [9, 10] and DFSZ [11, 12] frameworks. We provide in Section 4 cosmological bounds on flavor-violating axion couplings, and in Section 5 an updated cosmological bound on the QCD axion mass. We conclude in Section 6.

2. AXION DARK MATTER

The axion contribution to the observed dark matter relic density can be computed by analyzing the field evolution across the expansion history. At early times, at temperatures much higher than the QCD confinement scale, the finite-temperature axion potential is negligible and Hubble friction prevents any motion. The field starts evolving only when the primordial plasma temperature reaches values around the proton mass and the non-perturbative axion potential switches on. The resulting motion is described by damped harmonic oscillations around the minimum of the potential, and the amplitude of such oscillations gets damped by the Hubble expansion as non-relativistic dark matter. This is the misalignment production mechanism. The resulting energy density today depends on the axion decay constant and the initial field value. For the latter, we adopt the angular variable $\Theta = a/f_a$. An important interplay between the dynamics of PQ breaking and inflationary physics comes into play once one has to specify the initial field value Θ_0.

If the PQ phase transition happens after inflation, the two dynamics are decoupled and we can focus on PQ breaking only. The initial axion field value is selected randomly within each causal horizon at the PQ phase transition. Furthermore, when oscillations begin, the horizon size is much larger than the one at the PQ phase transition. Thus, we have different axion field values within a causal horizon, and one has to average over all possible initial field values Θ_0 that are uniformly distributed between $-\pi$ and π. This situation has the advantage that the axion relic density depends only on f_a. However, the misalignment contribution comes together with the one associated with topological defects formed at the PQ phase transition. Such a network of global axion strings formed at the PQ breaking scale must be evolved down to the nuclear scale. This is a multiscale problem as a consequence of the large mass hierarchy between the string core tension and the Hubble expansion rate; any numerical approach is extremely challenging. Unfortunately, such a prediction has generated conflicting results for decades, and an agreement is still not reached in the litera-

ture [13, 14, 15, 16, 17, 18]. The knowledge of how such a quantity depends on the axion microscopic parameters is extremely useful since it will allow us to target experimental searches appropriately.

On the contrary, if the PQ symmetry is broken during inflation and not restored afterward, the axion field is homogeneous within each causal horizon. Topological defects are inflated away for this case, and the resulting contribution from misalignment depends on both f_a and Θ_0. The results provided by [19] show the relation needed to reproduce the relic density.

3. AXION DARK RADIATION

A contribution to the cold dark matter abundance is far from being the only cosmological feature of PQ theories. The PQ framework leads to other fascinating phenomena in the early universe with testable consequences today. In what follows, we consider axions produced in the early universe with kinetic energy much larger than their rest mass. Several production mechanisms can be responsible for this additional population of hot axions. Regardless of the specific mechanism, their energy gets depleted with the expansion, and the overall energy density behaves as radiation as long as these axions remain relativistic. Thus, their effect is an additional contribution to the radiation energy density, and we measure this quantity by investigating the formation of light nuclei via Big Bang Nucleosynthesis (BBN) and the formation of the Cosmic Microwave Background (CMB). Historically, this effect has been quantified in terms of a modification of the total number of neutrino species. The effective number of neutrinos $N_{\rm eff}$ is related to the radiation energy density $\rho_{\rm rad}$ as

$$\rho_{\rm rad} = \rho_\gamma \left[1 + \frac{7}{8}\left(\frac{T_\nu}{T_\gamma}\right)^4 N_{\rm eff}\right]. \tag{4}$$

Any relativistic particle with a substantial energy density, like the axions, will contribute to $N_{\rm eff}$. We look for deviations from the standard cosmological value ($N_{\rm eff}^{\Lambda\rm CDM} = 3.044$):

$$\Delta N_{\rm eff} \equiv N_{\rm eff} - N_{\rm eff}^{\Lambda\rm CDM} = \frac{8}{7}\left(\frac{11}{4}\right)^{4/3}\frac{\rho_a}{\rho_\gamma}. \tag{5}$$

We focus here on thermal production channels. The QCD axion couples to gluons via the anomalous dimension 5 interaction given in equation (1). Couplings to other standard model particles are model dependent, and they are typically present (perhaps loop-suppressed) unless unnatural cancellations are in action. Thermal production is, in some sense, an unavoidable injection source since it only assumes the existence of a thermal bath at early times. For every specific model, the amount of axions produced thermally is determined unless we move away from a standard cosmological history. The leading production channels are binary scatterings and decays that produce relativistic axions because they are efficient above BBN, and they subsequently red-shift with the expansion until they get to the nonrelativistic regime. Such a transition can happen quite late. As a rule of thumb, the axion phase-space distribution stays thermal with a temperature not too much different from the ones of the radiation bath (given their thermal origin). Therefore, they manifest themselves as additional radiation at BBN if $m_a \lesssim$ MeV, and at recombination if $m_a \lesssim 0.3\,$eV.

We track the hot axion population in the early universe via the Boltzmann equation for the axion number density:

$$\frac{dn_a}{dt} + 3Hn_a = \gamma_a\left(1 - \frac{n_a}{n_a^{\rm eq}}\right). \tag{6}$$

The left hand simply accounts for the geometry of the expanding universe. The dynamics are on the right-hand side. Thus, our goal is to compute the so-called "collision terms" that account for all processes changing the number of axions between the initial and final state and solve the resulting Boltzmann equation. After interactions stop happening, the right-hand side vanishes and the comoving axion number density $Y_a = n_a/s$ reaches a constant value Y_a^∞. The resulting contribution to the additional neutrino species results in $\Delta N_{\rm eff} \simeq 74.85\,(Y_a^\infty)^{4/3}$.

One can compute the production rate for each one of the operators in equation (2) and then calculate the number of axions produced if we switch on a single operator at the time [20, 21, 22, 23, 24]. However, this situation is not always realistic because once we write down a UV complete model, multiple couplings contribute to axion production at different temperatures. Thus, we need the production rate across the entire expansion history to quantify axion production for specific UV complete models.

The study in [25] completed the calculation for the axion production rate at all temperatures for the two most popular classes of axion models: KSVZ [9, 10] and DFSZ [11, 12]. For the former, none of the standard model particles transforms under PQ, and the color anomaly is due to the presence of new heavy and colored fermions. For the latter, there are no new fermions in the spectrum, and the color anomaly is due to standard model quarks. A common feature of both frameworks, and actually of every UV complete model, is the presence of several mass thresholds across which the axion production rate changes its behavior drastically with the temperature. A threshold common to all PQ theories, which is a consequence of the interaction in equation (1) needed to solve the strong CP problem, is the QCD confinement scale. The analysis in [26] provided a continuous result for the production rate by extending previous calculations above such a scale and with a smooth interpolation in the between. Another mass threshold present within the KSVZ framework is the one associated with the heavy-colored fermions responsible for the anomaly; the operator in equation (1) is local only well below their masses, and the fermions themselves are dynamical degrees of freedom mediating axion production at higher temperatures. For the DFSZ case, the situation is ever richer due to the presence of several mass thresholds and the fact that all standard model particles are charged under PQ. First, this case features two Higgs doublets, and the mass scale of the heavy Higgs bosons has to be taken into account carefully since axion interactions are super-renormalizable at high temperatures. Furthermore, the electroweak phase transition is another important cosmological phase across which the rate changes its behavior with the temperature significantly as discussed in detail by [23].

The production rate for the KSVZ axion across the expansion history is illustrated in Figure 1. The mass of the heavy PQ-charge fermion is set to the value $m_\Psi = 10^5\,$GeV for illustration and consistently with collider bounds. We notice the different slope of the axion production rate above ($\gamma_a \propto T^4$) and below ($\gamma_a \propto T^6$) this mass threshold, and this is due to the fact that

above axion production is mediated by a renormalizable interaction. The scaling for temperatures below m_Ψ persists until the confinement scale where it drops exponentially due to the Maxwell-Boltzmann suppression for the pion number density.

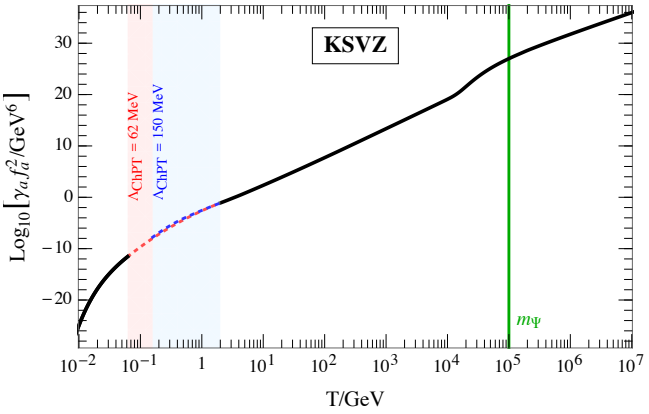

FIGURE 1: Production rate as a function of the temperature for the KSVZ axion (from [25]).

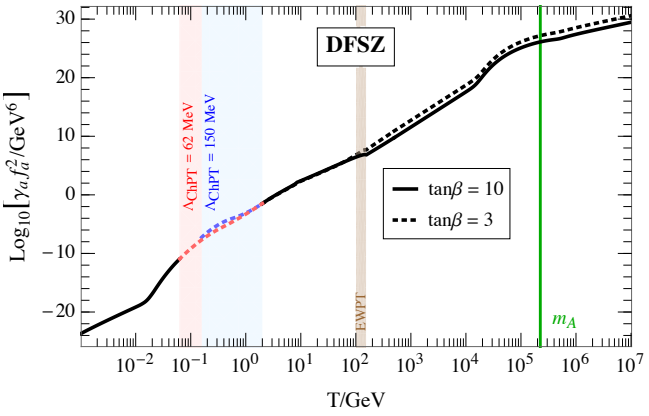

FIGURE 2: Production rate as a function of the temperature for the DFSZ axion (from [25]).

The analogous result for the DSFZ axion is illustrated in Figure 2. The mass of the heavy Higgs boson is also set at around the same scale, $m_A \simeq 10^5$ GeV, and the detailed choice of the additional parameter $\tan\beta$ (the ratio of the vacuum expectation values of the two Higgs fields) does not affect the rate appreciably. As anticipated above, the structure is even richer here. Similar to the previous case, axion production is mediated by a renormalizable operator at temperatures above m_A; the interaction is relevant in this case and therefore the rate scales as $\gamma_a \propto T^2$. Below the heavy Higgs bosons, dimension 5 coupling to standard model fermions (mostly top and bottom due to the larger Yukawa coupling) control the production rate that consequently scales as $\gamma_a \propto T^6$. Contrarily to the KSVZ case, fermion scatterings scaling as $\gamma_a \propto T^4$ dominate the production rate below the electroweak phase transition. Finally, pion scatterings are efficient as long as we do not hit the Maxwell-Boltzmann suppression. Nevertheless, axion production is active even well below the confinement scale since the axion couples to the muon and the electron.

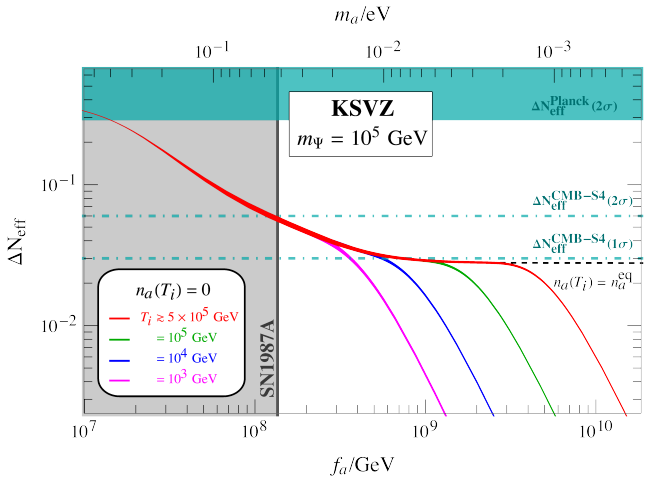

FIGURE 3: $\Delta N_{\rm eff}$ as a function of the axion decay constant for the KSVZ axion (from [25]).

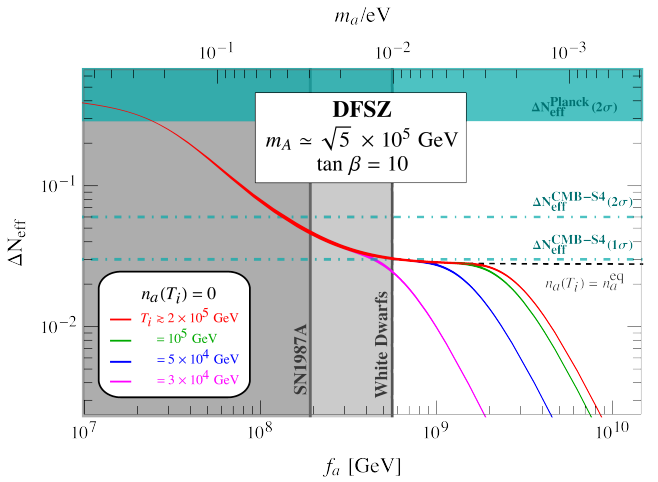

FIGURE 4: $\Delta N_{\rm eff}$ as a function of the axion decay constant for the DFSZ axion (from [25]).

We can insert this production rate into the Boltzmann equation in equation (6), and solve it to predict the amount of axion dark radiation expressed in terms of an effective number of additional neutrinos $\Delta N_{\rm eff}$. These predictions are shown in Figures 3 and 4 for the KSVZ and DFSZ axion, respectively. The parameter chosen for the model is specified in the legend, and different lines correspond to different temperatures where the Boltzmann code begins its evolution with vanishing axion population in the early universe. We notice how the region probed currently by Planck is already excluded by supernovae bounds; it is worth keeping in mind that these astrophysical bounds come with their caveats, and it is beneficial to have a complementary probe of that parameter space region. Future CMB-S4 surveys have the potential of probing unexplored regions of the parameter space. This is particularly true for the KSVZ axion whereas the CMB-S4 discovery reach for the DFSZ axion is around the same region as the one for white dwarf bounds (present because the DFSZ axion couples to the electron).

4. FLAVOR-VIOLATING AXION COUPLINGS

A broad class of theories widely explored in the recent literature is the one where axion couplings to standard model fermions are nondiagonal. The general Lagrangian capturing all models where this happens reads

$$\mathcal{L}_{\rm FV}^{(a)} = \frac{\partial_\mu a}{2f_a} \sum_{\psi_i \neq \psi_j} \bar{\psi}_i \gamma^\mu \left(c^V_{\psi_i\psi_j} + c^A_{\psi_i\psi_j} \gamma^5 \right) \psi_j . \tag{7}$$

These flavor-violating couplings arise in theories connecting the origin of the SM flavor structure with the PQ symmetry. Even if the high-scale theory preserves the flavor symmetry, they can arise from quantum corrections due to flavor-violating standard model interactions. They are the target of several terrestrial experiments searching for rare meson decays. The early universe offers a complementary probe for this class of theories as well. The analysis by [28] performed a systematic study of these flavor-violating couplings by switching one operator at a time. For the first time, the contribution from binary scatterings was included, and it was shown how it dominates completely the total axion production rate for the case of quarks. Scatterings were previously overlooked in the literature because decays always dominate unless there are hierarchies among the couplings mediating these processes. However, we can attach a QCD/QED interaction vertex to the three-point interactions in equation (7) and find a contribution proportional to the strong coupling constant. Furthermore, the treatment of the QCD crossover was improved via techniques analogous to the ones adopted for the flavor-conserving case.

The results in Figures 5 and 6 show the comparison between terrestrial and cosmological bounds for flavor-violating axion interactions with quarks and leptons, respectively. Dark bands are current bounds, and faint bands are projections for the future. The green bands (both dark and faint) show current and future cosmological bounds. For light quarks and leptons, we notice how laboratory searches perform better than cosmology. The situation changes once we include the third fermion generation where cosmology is competitive with terrestrial experiments and, in some cases, achieves better bounds.

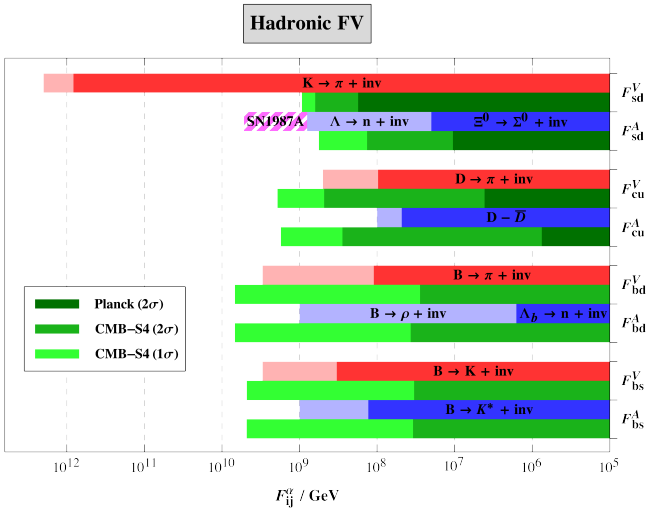

FIGURE 5: Current bounds and future prospects for flavor-violating axion interactions with quarks (figure from [28]).

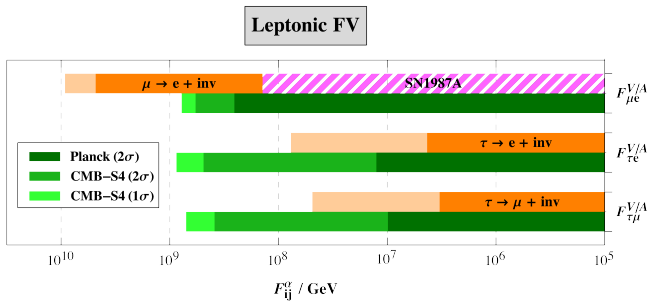

FIGURE 6: Current bounds and future prospects for flavor-violating axion interactions with leptons (figure from [28]).

5. UPDATED QCD AXION MASS BOUNDS

All the results presented so far neglected the axion mass. While this is definitely allowed at the time of BBN, it is not always the case at the time of recombination if the expression in equation (3) approaches values around 0.1 eV. The recent analysis by [29] incorporated a finite axion mass consistently, and the plots in Figures 7 and 8 show the outcome of such a complete cosmological analysis that included also baryon acoustic oscillations (BAO) for the KSVZ and DFSZ axion, respectively.

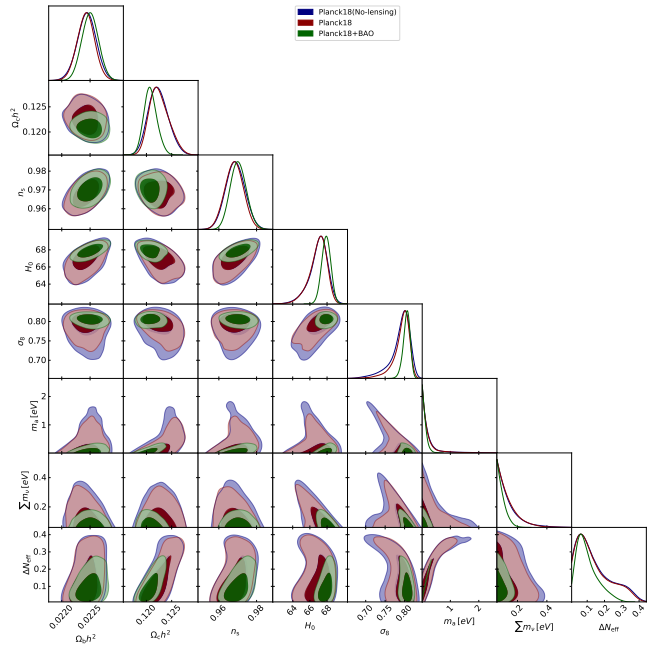

FIGURE 7: Allowed regions and one-dimensional probability posterior distributions for the KSVZ axion (figure from [29]).

We report the updated cosmological bounds on the axion mass

$$m_a \leq \begin{cases} 0.282\ (0.402)\ \text{eV} & \text{KSZV axion,} \\ 0.209\ (0.293)\ \text{eV} & \text{DFSZ axion.} \end{cases} \tag{8}$$

Here, the results are shown at 95% and 99% CL, and the bound is stronger for the DFSZ axion because it couples to all standard model particles and more production channels contribute. These bounds, obtained with the production rates of [25], are about a factor of 5 stronger than the ones found by previous analyses that adopted approximate results for the rates.

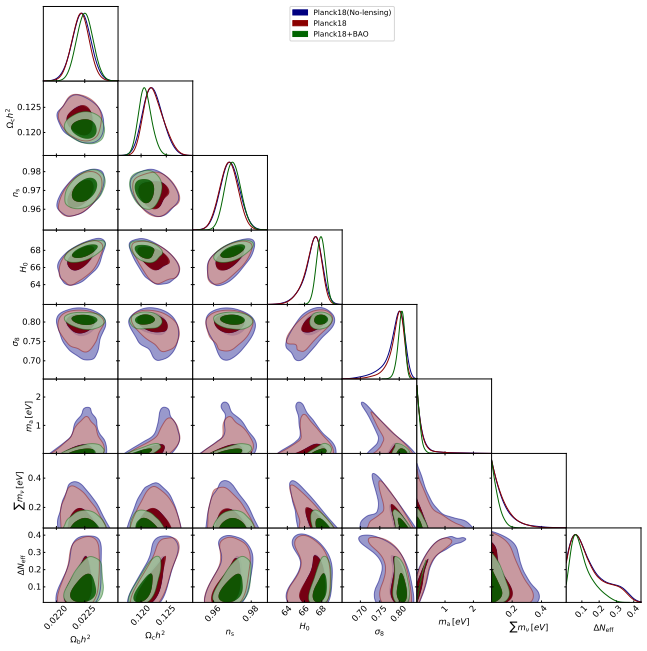

FIGURE 8: Allowed regions and one-dimensional probability posterior distributions for the DFSZ axion (figure from [29]).

6. OUTLOOK

The low-energy residual of the PQ framework, which is known as the QCD axion, kills two birds with one stone: the energy stored in the field oscillations behaves like cold dark matter. Axion detection is rather difficult because axion couplings are suppressed by the large PQ breaking scale. Besides searches in terrestrial laboratories, axion interactions lead to a plethora of rich phenomena in the early universe that leave an imprint in cosmological observables today. The production of cold dark matter is the reason why the QCD axion is one of the strongest motivated candidates from the top down, but it is far from being the only cosmological consequence of the PQ framework.

Thermal production of relativistic axions in the early universe is unavoidable if we have a thermal bath of standard model particles. This hot axion population leaves an imprint in the CMB for two broad classes of axion UV complete models. We point out also an intriguing interplay with flavor physics that we have just started to explore. The methodology presented here is general, and it can be employed to analyze other microscopic models such as explicit scenarios of flavor-violating couplings.

CONFLICTS OF INTEREST

The author declares that there are no conflicts of interest regarding the publication of this paper.

ACKNOWLEDGMENTS

This work was supported by "The Dark Universe: A Synergic Multi-messenger Approach" number 2017X7X85K under the program PRIN 2017 funded by the Ministero dell'Istruzione, Università e della Ricerca (MIUR) and "New Theoretical Tools for Axion Cosmology" under the Supporting TAlent in ReSearch@University of Padova (STARS@UNIPD). The author is supported by the Istituto Nazionale di Fisica Nucleare (INFN) through the Theoretical Astroparticle Physics (TAsP) project and by the European Union's Horizon 2020 research and innovation programme under the Marie Skłodowska-Curie grant agreement No. 860881-HIDDeN.

References

[1] R. D. Peccei and Helen R. Quinn. CP Conservation in the Presence of Instantons. *Phys. Rev. Lett.*, 38:1440–1443, 1977.

[2] R. D. Peccei and Helen R. Quinn. Constraints Imposed by CP Conservation in the Presence of Instantons. *Phys. Rev. D*, 16:1791–1797, 1977.

[3] Frank Wilczek. Problem of Strong P and T Invariance in the Presence of Instantons. *Phys. Rev. Lett.*, 40:279–282, 1978.

[4] Steven Weinberg. A New Light Boson? *Phys. Rev. Lett.*, 40:223–226, 1978.

[5] Giovanni Grilli di Cortona, Edward Hardy, Javier Pardo Vega, and Giovanni Villadoro. The QCD axion, precisely. *JHEP*, 01:034, 2016.

[6] John Preskill, Mark B. Wise, and Frank Wilczek. Cosmology of the Invisible Axion. *Phys. Lett. B*, 120:127–132, 1983.

[7] L. F. Abbott and P. Sikivie. A Cosmological Bound on the Invisible Axion. *Phys. Lett. B*, 120:133–136, 1983.

[8] Michael Dine and Willy Fischler. The Not So Harmless Axion. *Phys. Lett. B*, 120:137–141, 1983.

[9] Jihn E. Kim. Weak Interaction Singlet and Strong CP Invariance. *Phys. Rev. Lett.*, 43:103, 1979.

[10] Mikhail A. Shifman, A. I. Vainshtein, and Valentin I. Zakharov. Can Confinement Ensure Natural CP Invariance of Strong Interactions? *Nucl. Phys. B*, 166:493–506, 1980.

[11] A. R. Zhitnitsky. On Possible Suppression of the Axion Hadron Interactions. (In Russian). *Sov. J. Nucl. Phys.*, 31:260, 1980.

[12] Michael Dine, Willy Fischler, and Mark Srednicki. A Simple Solution to the Strong CP Problem with a Harmless Axion. *Phys. Lett. B*, 104:199–202, 1981.

[13] Marco Gorghetto, Edward Hardy, and Giovanni Villadoro. Axions from Strings: the Attractive Solution. *JHEP*, 07:151, 2018.

[14] Marco Gorghetto, Edward Hardy, and Giovanni Villadoro. More axions from strings. *SciPost Phys.*, 10(2):050, 2021.

[15] Malte Buschmann, Joshua W. Foster, and Benjamin R. Safdi. Early-Universe Simulations of the Cosmological Axion. *Phys. Rev. Lett.*, 124(16):161103, 2020.

[16] Malte Buschmann, Joshua W. Foster, Anson Hook, Adam Peterson, Don E. Willcox, Weiqun Zhang, and Benjamin R. Safdi. Dark matter from axion strings with adaptive mesh refinement. *Nature Commun.*, 13(1):1049, 2022.

[17] Vincent B. Klaer and Guy D. Moore. How to simulate global cosmic strings with large string tension. *JCAP*, 10:043, 2017.

[18] Vincent B. Klaer and Guy D. Moore. The dark-matter axion mass. *JCAP*, 11:049, 2017.

[19] Sz. Borsanyi et al. Calculation of the axion mass based on high-temperature lattice quantum chromodynamics. *Nature*, 539(7627):69–71, 2016.

[20] Ricardo Z. Ferreira and Alessio Notari. Observable Windows for the QCD Axion Through the Number of Relativistic Species. *Phys. Rev. Lett.*, 120(19):191301, 2018.

[21] Francesco D'Eramo, Ricardo Z. Ferreira, Alessio Notari, and José Luis Bernal. Hot Axions and the H_0 tension. *JCAP*, 11:014, 2018.

[22] Fernando Arias-Aragón, Francesco D'Eramo, Ricardo Z. Ferreira, Luca Merlo, and Alessio Notari. Cosmic Imprints of XENON1T Axions. *JCAP*, 11:025, 2020.

[23] Fernando Arias-Aragón, Francesco D'Eramo, Ricardo Z. Ferreira, Luca Merlo, and Alessio Notari. Production of Thermal Axions across the ElectroWeak Phase Transition. *JCAP*, 03:090, 2021.

[24] Daniel Green, Yi Guo, and Benjamin Wallisch. Cosmological implications of axion-matter couplings. *JCAP*, 02(02):019, 2022.

[25] Francesco D'Eramo, Fazlollah Hajkarim, and Seokhoon Yun. Thermal QCD Axions across Thresholds. *JHEP*, 10:224, 2021.

[26] Francesco D'Eramo, Fazlollah Hajkarim, and Seokhoon Yun. Thermal Axion Production at Low Temperatures: A Smooth Treatment of the QCD Phase Transition. *Phys. Rev. Lett.*, 128(15):152001, 2022.

[27] Kyu Jung Bae, Kiwoon Choi, and Sang Hui Im. Effective Interactions of Axion Supermultiplet and Thermal Production of Axino Dark Matter. *JHEP*, 08:065, 2011.

[28] Francesco D'Eramo and Seokhoon Yun. Flavor violating axions in the early Universe. *Phys. Rev. D*, 105(7):075002, 2022.

[29] Francesco D'Eramo, Eleonora Di Valentino, William Giarè, Fazlollah Hajkarim, Alessandro Melchiorri, Olga Mena, Fabrizio Renzi, and Seokhoon Yun. Cosmological bound on the QCD axion mass, redux. *JCAP*, 09:022, 2022.